Determination of the Spectral Absorption of Solar Radiation by Marine Stratocumulus Clouds from Airborne Measurements within Clouds

MICHAEL D. KING

Laboratory for Atmospheres, Goddard Space Flight Center, NASA, Greenbelt, Maryland

LAWRENCE F. RADKE AND PETER V. HOBBS

Department of Atmospheric Sciences, University of Washington, Seattle, Washington

(Manuscript received 8 June 1989, in final form 9 November 1989)

ABSTRACT

A multiwavelength scanning radiometer has been used to measure the angular distribution of scattered radiation deep within a cloud layer at discrete wavelengths between 0.5 and 2.3 μm. The relative angular distribution of the intensity field at each wavelength is used to determine the similarity parameter, and hence single scattering albedo, of the cloud at that wavelength using the diffusion domain method. In addition to the spectral similarity parameter, the analysis provides a good estimate of the optical thickness of the cloud *beneath* the aircraft. Results of such analysis are presented for a 50 km section of clean marine stratocumulus clouds off the coast of California on 10 July 1987. These observations were obtained from the University of Washington Convair C-131A aircraft as part of the First ISCCP (International Satellite Cloud Climatology Project) Regional Experiment (FIRE). In addition to the radiation measurements, we obtained microphysical and thermodynamic measurements from which the expected similarity parameter spectrum was calculated using accepted values of the refractive index of liquid water and the transmission function of water vapor. The measured absorption for this case of clean maritime clouds is close to, but persistently larger than, theoretical predictions. Finally, measurements are presented of the spectral albedo of the ocean surface under overcast conditions.

1. Introduction

Although the importance of clouds on the radiation balance of the earth is widely recognized (Ramanathan 1987; Ramanathan et al. 1989), interactions of solar radiation with clouds is one of the weakest links in our understanding of the global climate system. It is also now recognized that a knowledge of cloud properties and their variation in space and time is crucial to studies of global climate change, such as trace gas greenhouse effects (Cess et al. 1989). As general circulation model (GCM) simulations become more sophisticated in their treatment of shortwave cloud radiative properties, through incorporation of parameterizations in terms of liquid water path and cloud droplet size (Slingo 1989), it becomes increasingly important to examine how well observations and theory are in agreement.

The absorption of solar radiation by clouds is governed by the optical thickness, single scattering albedo, and phase function of the cloud, as well as the albedo of the underlying surface and the water vapor distribution of the environment in which the cloud is located. Theoretical calculations suggest that water clouds can absorb up to 15%–20% of the incident solar radiation, with the largest values arising from the thickest clouds with large cloud droplets, an overhead sun, and little water vapor above the cloud (Twomey 1976; Slingo and Schrecker 1982; Davies et al. 1984; Stephens et al. 1984; Wiscombe et al. 1984; Slingo 1989). In addition to the total cloud absorption, calculations also show that heating rates near cloud top can reach 2 K h^{-1}, and thus contribute significantly to the sudden "burning off" of California stratus layers as the solar zenith angle decreases towards noon (Twomey 1983).

The majority of cloud absorption observations to date have involved interpreting broadband pyranometer measurements acquired from research aircraft flown above and below clouds. All of these observations have involved single aircraft missions in which it is exceedingly difficult to obtain comparable flux observations above and below the same cloud layer. In spite of these difficulties, aircraft pyranometer observations by Reynolds et al. (1975), Herman (1977), Stephens et al. (1978), Herman and Curry (1984), Hignett (1987) and Foot (1988) have generally shown a systematic discrepancy between measurements and theory, whereby measurements of the absorption of solar radiation by clouds are generally larger than theoretical

Corresponding author address: Dr. Michael D. King, Laboratory for Atmospheres, Goddard Space Flight Center/NASA, Code 913 Greenbelt, MD 20771.

predictions or, alternatively, the near-infrared albedo measurements are generally smaller than theory. Unexpectedly low measurements of the reflection of solar radiation by clouds have also been reported by Rozenberg et al. (1974), Twomey and Cocks (1982), Stephens and Platt (1987), and Foot (1988) using spectral reflectance measurements.

As a consequence of these reported discrepancies between measurements and theory, as well as the widely recognized limitation of single aircraft broadband pyranometer observations, we were prompted to develop the diffusion domain method for determining the spectral absorption of solar radiation by clouds (King 1981). In this method, the intensity of scattered radiation deep within a cloud layer is measured as a function of zenith angle for selected wavelengths in the visible and near-infrared. In the diffusion domain region of an optically thick medium, located sufficiently far from the top and bottom boundaries of the medium (cloud), the intensity distribution is azimuthally independent and monotonically decreasing from zenith to nadir, with the relative angular distribution independent of the solar zenith angle and a strong function of the similarity parameter (and hence single scattering albedo).

The intent of this paper is to present the first aircraft observations of the scattered radiation field inside clouds, together with an analysis of the spectral similarity parameter derived from these measurements using the diffusion domain method. The data were obtained using the multiwavelength scanning radiometer described by King et al. (1986), which flew on the University of Washington's Convair C-131A aircraft during the marine stratocumulus intensive field observation component of FIRE, conducted off the coast of San Diego, California during July 1987. The microphysical structure of the clouds, including cloud droplet size distributions, were also monitored continuously with instruments aboard the aircraft.

In this paper, we briefly review the diffusion domain method for deriving the cloud similarity parameter and present an analysis of the results obtained for a 50 km section of marine stratocumulus cloud on 10 July 1987. In addition to the observations, we will emphasize the quality control tests required to select those portions of an aircraft flight for which measurements are obtained within the diffusion domain. Finally, we will present a comparison of the experimentally derived similarity parameter spectrum with that expected theoretically from the cloud droplet size distribution measured simultaneously from the aircraft.

2. Diffusion domain method

From a position deep within an optically thick and horizontally extensive cloud layer, it is possible to derive quantitative information about cloud absorption properties from the angular distribution of scattered radiation (King 1981). Within this region, known as the diffusion domain, the diffuse radiation field assumes an asymptotic form characterized by rather simple properties. For a vertically homogeneous cloud layer at a wavelength for which the single scattering albedo $\omega_0 < 1$, the intensity in the diffusion domain is azimuthally independent and given by

$$I(\tau, u) = s_1 P(u) e^{-k\tau} + s_2 P(-u) e^{-k(\tau_c - \tau)}. \quad (1)$$

In this expression τ is the optical thickness measured from the upper boundary of the cloud, τ_c the total optical thickness of the cloud, u the cosine of the zenith angle with respect to the positive τ direction ($-1 \leq u \leq 1$), $P(u)$ the diffusion pattern (eigenfunction), k the diffusion exponent (eigenvalue), and s_1 and s_2 the strengths of the diffusion streams in the positive and negative τ directions, respectively.

Under the assumption that the cloud layer overlies a surface that reflects radiation according to Lambert's law with a total reflectivity A_g, it can be shown (King 1981) that

$$s_1 = \frac{\mu_0 F_0 (1 - A_g A^*) K(\mu_0)}{\pi[(1 - A_g A^*)(1 - f^2) + A_g m n^2 l e^{-2k\tau_c}]}, \quad (2)$$

$$s_2 = -\left[l - \frac{A_g m n^2}{1 - A_g A^*}\right] s_1 e^{-k\tau_c}, \quad (3)$$

where

$$f = l e^{-k\tau_c}. \quad (4)$$

In addition to the cosine of the solar zenith angle μ_0 and the incident solar flux density F_0, the magnitudes of the diffusion streams s_1 and s_2 are seen to depend on the escape function $K(\mu_0)$ as well as the asymptotic constants A^*, m, n, and l.

The functions and constants that appear in (1)–(4) can be obtained by applying the asymptotic fitting method of van de Hulst (1968), whereby numerical computations from the doubling method are fit to known asymptotic formulae for the plane albedo and total transmission of thick layers. Illustrations of these functions and constants can be found in King (1981, 1987) and King and Harshvardhan (1986) for phase functions representative of clouds at visible and near-infrared wavelengths.

Of primary significance for the determination of cloud absorption properties, however, is the fact that the *relative* angular distribution of scattered radiation is independent of the solar zenith angle and solar flux density and only dependent on the optical properties of the medium (cloud) and the total reflectivity of the underlying surface. Substituting (3) into (1), King (1981) showed that the ratio of the nadir-to-zenith intensities within the diffusion domain is given by:

$$\frac{I(\tau,-1)}{I(\tau,1)}=\frac{(1-A_gA^*)[D-le^{-2k(\tau_c-\tau)}]+A_gmn^2e^{-2k(\tau_c-\tau)}}{(1-A_gA^*)[1-Dle^{-2k(\tau_c-\tau)}]+A_gmn^2De^{-2k(\tau_c-\tau)}}. \tag{5}$$

The diffusion pattern ratio D, defined by:

$$D=P(-1)/P(1), \tag{6}$$

represents the ratio of the nadir-to-zenith intensities within the diffusion domain of an infinitely thick atmosphere, and is an upper limit to the intensity ratio that can be achieved in clouds.

The strength of the diffusion domain method lies in the fact that the asymptotic constants l, n m, D, A^*, and k that appear in (5) are strongly dependent on ω_0, with a somewhat weaker dependence on the asymmetry factor g. Though one might expect each constant to depend on all the coefficients in the Legendre polynomial expansion of the phase function, it turns out that these constants can be well described by a function of a similarity parameter s, defined by:

$$s=\left(\frac{1-\omega_0}{1-\omega_0 g}\right)^{1/2}, \tag{7}$$

where s reduces to $(1-\omega_0)^{1/2}$ for isotropic scattering and spans the range 0 ($\omega_0=1$) to 1 ($\omega_0=0$).

Similarity relations for the asymptotic constants that arise in the diffusion domain method are summarized in Table 1. With the exception of $k/(1-g)$, these formulas are accurate for all asymmetry factors, as demonstrated by King (1981). The formula for $k/(1-g)$ is strictly valid over the narrower range of asymmetry factors that occur in terrestrial clouds at visible and near-infrared wavelengths (viz., $0.8 \leqslant g \leqslant 0.9$). A more general similarity relation for $k/(1-\omega_0 g)$ applicable for all asymmetry factors can be found in King and Harshvardhan (1986). As a consequence of these similarity relations, the ratio of the nadir-to-zenith intensities in the diffusion domain is seen to be solely a function of the surface reflectivity (A_g), similarity parameter (s), and scaled optical thickness *beneath* the level of the observations $[(1-g)(\tau_c-\tau)]$.

TABLE 1. Similarity relations satisfied by constants that arise in the diffusion domain method for determining the spectral similarity parameter of clouds.

$$l=\frac{(1-0.6813s)(1-s)}{(1+0.7919s)}$$

$$n=\left[\frac{(1+0.4142s)(1-s)}{(1+1.8877s)}\right]^{1/2}$$

$$m=(1+1.537s)\ln\left[\frac{1+1.800s-7.087s^2+4.740s^3}{(1-0.819s)(1-s)^2}\right]$$

$$D=\frac{(1-0.9874s)(1-s)}{(1+1.4767s)}$$

$$A^*=\frac{(1-0.1464s)(1-s)}{(1+1.1629s)}$$

$$k/(1-g)=(1+0.4426s)\ln\left[\frac{(1+2.8162s)}{(1+2.0785s)(1-s)}\right]$$

ω_0 single scattering albedo
g asymmetry factor
s similarity parameter $[(1-\omega_0)/(1-\omega_0 g)]^{1/2}$

For conservative scattering the asymptotic expression for the internal scattered radiation field given by (1) is indeterminate, since $P(u)=n=l=1$ and $m=k=0$. Expanding these functions to first order in s, King (1981) has shown that (1) can be rewritten as:

$$I(\tau,u)=\frac{\mu_0F_0K(\mu_0)}{\pi[3(1-A_g)(1-g)(\tau_c+2q_0)+4A_g]}\times\{3(1-A_g)[(1-g)(\tau_c-\tau+q_0)+u]+4A_g\}, \tag{8}$$

where q_0 is the extrapolation length. The reduced extrapolation length $q'=(1-g)q_0$ ranges between 0.709 and 0.715 for all possible phase functions (van de Hulst 1980), but for anisotropic cloud phase functions it can be well approximated by 0.714 (King 1981).

As we will see in subsequent sections, Eq. (8) is an extremely useful relationship because it predicts that the angular distribution of the intensity field in the diffusion domain at a nonabsorbing wavelength is of the form $I(\tau,\cos\theta)=a+b\cos\theta$, where θ is the zenith angle ($u=\cos\theta$). Furthermore, (8) shows that the radiation field becomes more isotropic as the optical thickness and surface reflectivity increase. Thus, if we can obtain diffusion domain measurements at a nonabsorbing wavelength for which (8) is satisfied, it follows that the ratio of the nadir-to-zenith intensities is given by:

$$\frac{I(\tau,-1)}{I(\tau,1)}=\frac{3(1-A_g)[(1-g)(\tau_c-\tau+q_0)-1]+4A_g}{3(1-A_g)[(1-g)(\tau_c-\tau+q_0)+1]+4A_g}. \tag{9}$$

Since $q'\approx 0.714$, this expression shows that the internal intensity ratio for conservative scattering is reduced to a function solely of A_g and $(1-g)(\tau_c-\tau)$. Solving (9) for the scaled optical thickness $\tau_c'-\tau'$ yields:

$$\tau_c'-\tau'=(1-g)(\tau_c-\tau)=\frac{I(\tau,1)+I(\tau,-1)}{I(\tau,1)-I(\tau,-1)}-q'-\frac{4A_g}{3(1-A_g)}. \tag{10}$$

Thus, by measuring the intensities in the zenith $[I(\tau,1)]$ and nadir $[I(\tau,-1)]$ directions with the same instrument, it is straightforward to calculate the scaled

optical thickness beneath the aircraft flight level if the total reflectivity of the surface is known. In this way, it is unnecessary to know the extraterrestrial solar flux density, solar zenith angle, or absolute calibration of the instrument precisely, as these parameters affect only the magnitude of the intensity field and not the relative angular distribution.

With $(1 - g)(\tau_c - \tau)$ thus determined from an intensity ratio measurement at a visible (nonabsorbing) wavelength, the similarity parameter s can be determined as a function of wavelength from intensity ratio measurements at other wavelengths where the cloud absorbs solar radiation. By making use of the similarity relations given in Table 1, together with Eq. (5), the intensity ratio at these wavelengths can be calculated as a function of s. We have made use of spline interpolation to invert these calculations in order to determine the similarity parameter that agrees best with the internal intensity ratio measurements.

To relate spectral values of the similarity parameter to the physically important parameter ω_0, it is necessary to determine the asymmetry factor g. For a water cloud this can be accomplished by measuring the cloud droplet size distribution from the same aircraft platform as that from which the radiation measurements are made, thereby permitting g to be computed. In fact, for a successful implementation of the diffusion domain method it is necessary to allow the scaled optical thickness determined from (10) to vary as a function of wavelength. Furthermore, it is necessary to measure the total reflectivity of the surface as a function of wavelength. Finally, and of perhaps greatest importance, it is necessary to be able to determine from the measurements themselves whether the conditions of the diffusion domain are satisfied. These practical considerations will be addressed in some detail in the following sections, where we present our analysis of observations obtained in marine stratocumulus clouds off the coast of San Diego during July 1987.

3. Spectral properties of cloud layers

Hansen and Travis (1974) were the first to establish that the single scattering properties of a polydisperse distribution of particles are largely insensitive to the shape of the size distribution, depending instead on the effective radius r_e, and, to a lesser extent, a dimensionless effective variance v_e, defined by:

$$r_e = \int_0^\infty r^3 n(r)dr \Big/ \int_0^\infty r^2 n(r)dr \qquad (11)$$

$$v_e = \int_0^\infty (r - r_e)^2 r^2 n(r)dr \Big/ \int_0^\infty r_e^2 r^2 n(r)dr. \qquad (12)$$

In these expressions $n(r)$ is the particle size distribution, which is a function of particle radius r.

Before applying the diffusion domain method to experimental measurements of the internal scattered radiation field, it is instructive to examine the spectral dependence of the optical thickness, asymmetry factor, scaled optical thickness, and similarity parameter of water clouds for selected values of the effective radius. These results, presented in Figs. 1–4, were calculated from Mie theory and are based on spherical water droplets having the complex refractive indices tabulated by Hale and Querry (1973) for wavelengths in the range $0.25 \leq \lambda \leq 0.69$ μm, Palmer and Williams (1974) for $0.69 < \lambda \leq 2.0$ μm, and Downing and Williams (1975) for $\lambda > 2.0$ μm. Furthermore, we have assumed that the cloud drop size distribution is a modified gamma distribution of the form (Hansen 1971):

$$n(r) = Cr^{(1 - 3v_e)} \exp\left(-\frac{r}{r_e v_e}\right), \qquad (13)$$

with $v_e = 0.111$.

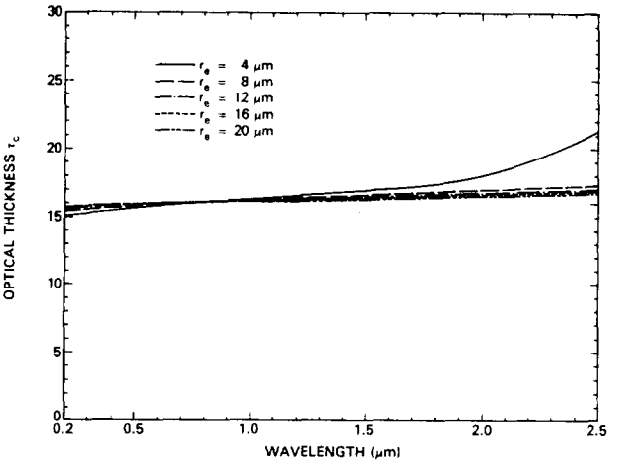

FIG. 1. Cloud optical thickness as a function of wavelength for selected values of the effective radius. Results apply to water clouds having a modified gamma size distribution with an effective variance $v_e = 0.111$.

Although we have scaled the calculations to make the optical thickness at 0.754 μm the same for all values of the effective radius, Fig. 1 shows that τ_c is nearly independent of wavelength. The optical thickness increases significantly with increasing wavelength only when the wavelength approaches r_e, as is the case in this figure for $r_e = 4$ μm and $\lambda \gtrsim 2$ μm. This is a direct consequence of the first peak in the Mie extinction efficiency factor. The asymmetry factor, scaled optical thickness, and similarity parameter, on the other hand, vary significantly with both wavelength and effective radius (cf. Figs. 2–4). A careful examination of Figs. 2 and 4 reveals that at 0.5 μm, where the similarity parameter is nearly zero, the asymmetry factor increases with increasing radius in accord with Mie theory predictions for conservative scattering. The enhanced values of the asymmetry factor near 1.44 and 1.93 μm arise from the significant absorption of solar radiation by cloud droplets at these wavelengths (cf. Fig. 4), which has the effect of reducing the backscattering.

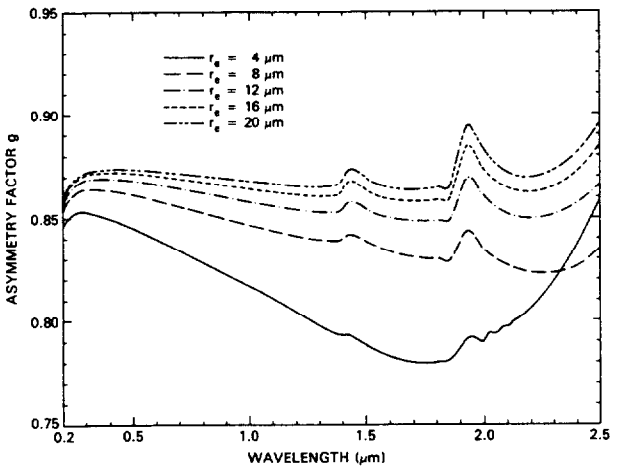

FIG. 2. As in Fig. 1 except for the asymmetry factor of the cloud droplets.

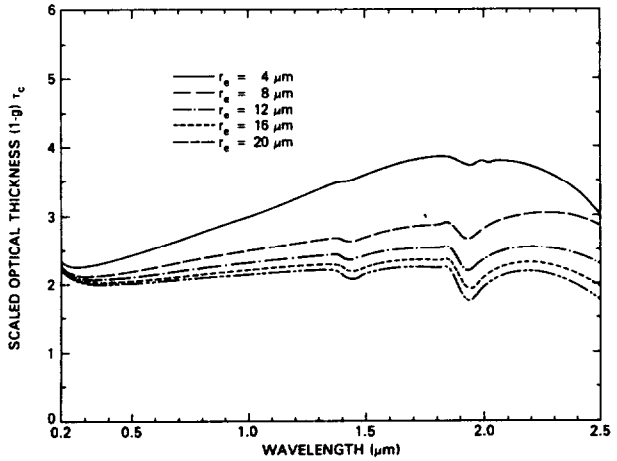

FIG. 3. As in Fig. 1 except for the scaled optical thickness.

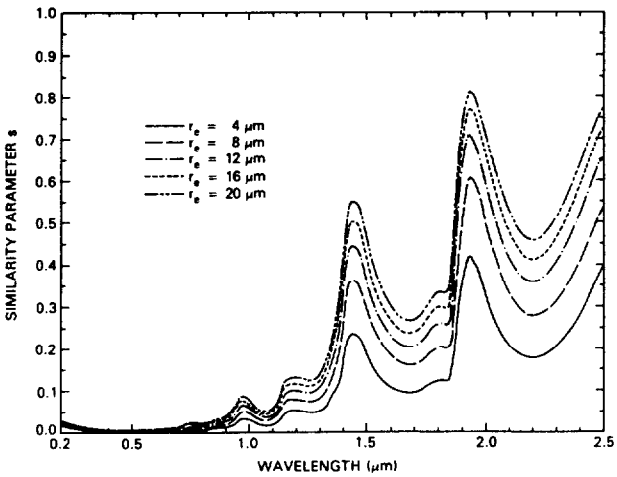

FIG. 4. As in Fig. 1 except for the similarity parameter.

Although the diffusion domain method, in its simplest form, requires the assumption that the cloud is nonabsorbing at some wavelength in the visible region (e.g., 0.5 μm), this assumption is necessary solely for the purpose of estimating the scaled optical thickness between the aircraft flight level and the base of the cloud [Eq. (10)]. Since this parameter becomes less important as the optical thickness increases and as the similarity parameter (absorption) increases, this assumption is expected to have little influence on the derived similarity parameter at wavelengths in the near-infrared. On the other hand, the results presented in Fig. 3 clearly show that $\tau_c' - \tau'$ varies significantly with wavelength and cloud droplet size. This spectral variation must be taken into account in order to estimate the similarity parameter in the weakly absorbing wavelengths in the vicinity of 0.5 μm. Since this spectral variation depends on the drop size distribution in the cloud, it is necessary to measure the cloud drop size distribution simultaneously with the measurements of scattered solar radiation within the cloud.

4. Diffusion domain measurements

The measurements required to implement the theory described above can be obtained with the cloud absorption radiometer (CAR). This instrument, described in detail by King et al. (1986), is a 13-channel scanning radiometer that is mounted in the nose of the University of Washington's Convair C-131A research aircraft. The instrument scans in a vertical plane on the right-hand side of the aircraft from 5° before zenith to 5° past nadir (190° aperture). This permits observations of both the zenith and nadir intensities with as much as a 5° aircraft roll, an angle that was measured simultaneously with a gyroscope aboard the aircraft.

The first seven channels of the CAR are continuously and simultaneously sampled, while the eighth registered channel is selected from among the six channels on a filter wheel. With automatic sequencing the filter wheel rotates to a new filter position every fourth scan. Since the scan rate of the radiometer is 1.67 Hz, each minute of flight duration results in 100 measurements of the angular intensity field for each of the first seven channels and typically 12 measurements for each of the six filter wheel channels. At our nominal aircraft speed of 80 m s^{-1}, it follows that the zenith and nadir intensity measurements are obtained within a distance of approximately 24 m for each scan of the radiometer.

Figure 5 illustrates the location of the C-131A flight track between 0922 and 0955 PDT (1622 and 1655 UTC) on 10 July 1987. We will now present and discuss the internal scattered radiation measurements acquired by the CAR in the central 50 km of this flight line, denoted by the solid line in Fig. 5. These observations, acquired between 0931 and 0941 PDT, were located approximately 355 km from the airfield on

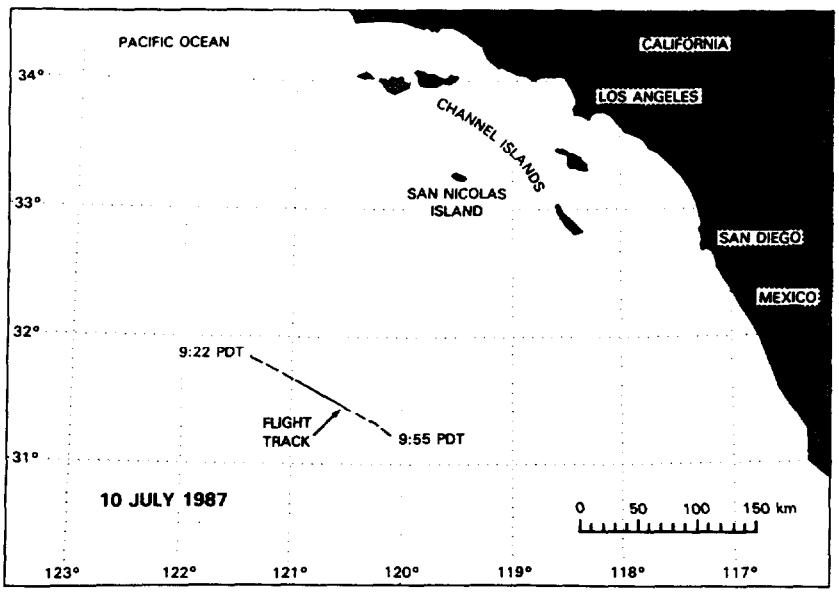

FIG. 5. Location of the C-131A flight track between 0922 and 0955 PDT on 10 July 1987. The central 50 km of this flight line, denoted by a solid line, is the section of marine stratocumulus cloud analyzed in this study.

Coronado Island, San Diego. They represent one of the aircraft missions flown during the marine stratocumulus intensive field observation component of FIRE. A general description of FIRE and the associated IFOs is given by Cox et al. (1987), with a detailed summary of the marine stratocumulus IFO provided by Albrecht et al. (1988).

Figure 6 shows the relative intensity $I(\tau, \cos\theta)/I(\tau, 1)$ as a function of zenith angle θ for selected wavelengths of the cloud absorption radiometer. These measurements were obtained near 0937 PDT (29.2 km from the start of the CAR measurements at 0931 PDT), with the scans at two of the filter wheel channels (1.64 and 2.20 μm) coming from scans within 26 s (2.2 km) of the remainder of the scans. We believe these measurements represent the first angular intensity measurements of scattered radiation within a cloud. Aside from the quantization (digitization) noise at the shortest wavelengths and the instrumental (electrical) nose at the longest wavelengths, two main features are seen in Fig. 6. These are 1) the angular intensity field at the shortest wavelength follows very nearly the cosine function expected for conservative scattering in the diffusion domain [cf. Eq. (8)], and 2) the angular intensity field becomes increasingly anisotropic as absorption increases. This is especially noticeable at 2.00 μm, the wavelength in the instrument where water has the greatest absorption. The experimental observations presented in Fig. 6 complement a comparable theoretical figure (for selected values of the similarity parameter rather than wavelength) presented in King et al. (1986).

Figure 7 illustrates the zenith and nadir intensities as a function of distance (time) for measurements obtained inside clouds. These data, corresponding to observations at $\lambda = 0.503$ μm, show that the zenith and nadir intensities are quite uniform within these clouds.

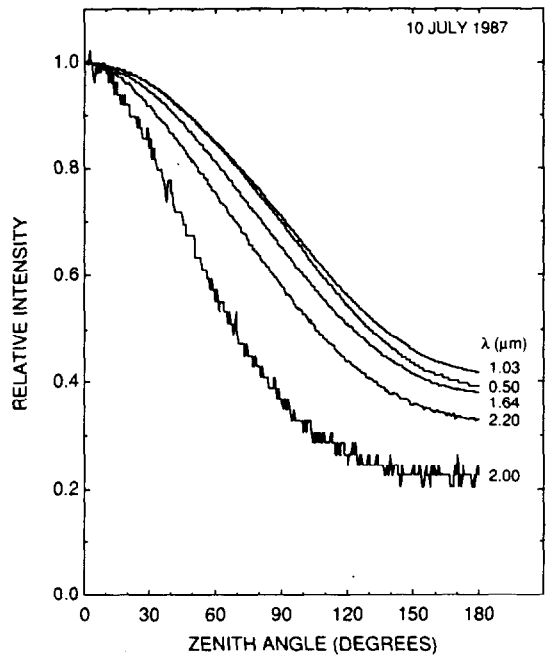

FIG. 6. Relative intensity as a function of zenith angle and wavelength for internal scattered radiation measurements obtained with the cloud absorption radiometer at 0937 PDT.

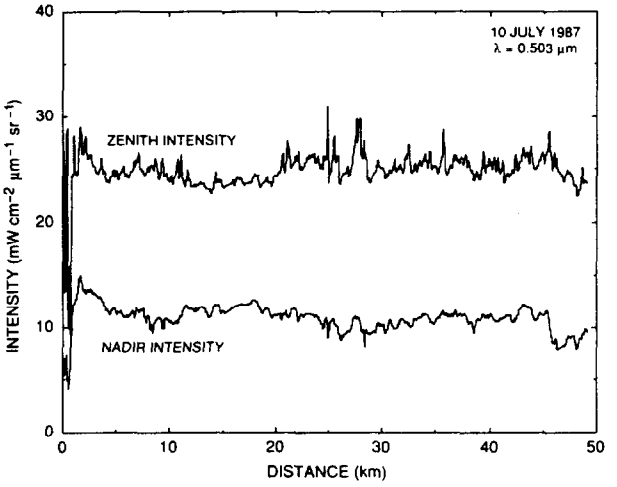

FIG. 7. Zenith and nadir intensities as a function of distance along the flight track for measurements obtained inside the clouds between 0941 and 0951 PDT. These measurements were obtained at a wavelength $\lambda = 0.503$ μm.

The scan lines illustrated in Fig. 6 were obtained between distances of 27.1 and 31.2 km of Fig. 7. A careful examination of Fig. 7 suggests that the cloud near the start of the flight line is too optically thin to have a diffusion domain, as evidenced by very low zenith and nadir intensity measurements. Furthermore, the measurements near 24.9 and 28.0 km, though probably in a cloud of sufficient optical thickness to have a diffusion domain, were obtained too near the cloud top, so the zenith measurements were contaminated by directly transmitted solar radiation.

The determination of the cloud similarity parameter is based on making measurements of the ratio of the nadir-to-zenith intensities within the diffusion domain of an optically thick cloud. In order to determine which measurements presented in Fig. 7 are within the diffusion domain, we have developed a comprehensive set of tests to which the CAR data are subjected.

In channel 1 ($\lambda = 0.503$ μm), where the cloud is expected to have a small to negligible amount of absorption, the angular distribution of the radiation field obtained from measurements is compared to that expected in the diffusion domain for conservative scattering [viz., $I(\tau, \cos\theta) = a + b\cos\theta$]. In particular, the measured intensities in the zenith [$I(\tau, 1)$] and nadir [$I(\tau, -1)$] directions are obtained (e.g., Fig. 7), from which the theoretical function $I(\tau, \cos\theta) = a + b\cos\theta$ is constructed, where

$$a = \frac{1}{2}[I(\tau, 1) + I(\tau, -1)], \tag{14}$$

$$b = \frac{1}{2}[I(\tau, 1) - I(\tau, -1)]. \tag{15}$$

The individual measurements in the range $0° \leq \theta \leq 180°$ are then compared with this curve, as illustrated in Fig. 8 for both a satisfactory (Fig. 8a) and unsatisfactory (Fig. 8b) scan. Superimposed on the measurements (continuous curve) is the theoretical cosine function (dashed curve) necessary for the measurements to be within the diffusion domain. To highlight the similarities and differences between these two results, the lower portion of Fig. 8 shows the deviations between measurements and theory as a function of zenith angle. These latter results apply to the right-hand scale. Measurements from an individual scan of the CAR are considered to be in the diffusion domain if *all* of the following quality control tests are satisfied:

(i) The zenith intensity exceeds the nadir intensity.

(ii) The maximum deviation from the theoretical (cosine) curve is less than or equal to 5% of the mean amplitude.

(iii) The sample standard deviation around the theoretical curve is either 1) less than or equal to 1.25%, or 2) between 1.25% and 2.5%, and the number of times the deviations $\epsilon_i = I(\quad \cos\theta_i) - a - b\cos\theta_i$ change sign is greater than or equal to 4. This test assures that the fluctuations of the data around the theoretically expected cosine curve have random fluctuations, rather than large systematic drifts (as in Fig. 8b).

An individual scan line of data is only subjected to these quality control tests if the aircraft roll is less than or equal to 5°, thereby enabling both the zenith and nadir intensities to be measured.

On 10 July 1987 our tests showed that a staggering 3133 scans (over a period of 31.3 min and a flight path of 155 km) met these criteria and were therefore suitable for derivation of the similarity parameter of clouds using the diffusion domain method.

5. Results from observations on 10 July 1987

Once the portions of a flight containing diffusion domain measurements have been identified, it is rather straightforward to analyze the measurements to derive the spectral similarity parameter of clouds using the diffusion domain method. This analysis requires ancillary information on the spectral surface reflectivity, which we derived from 96 scans (~1 min) of the CAR obtained beneath the stratocumulus cloud layer at 1145 PDT. We assumed the transmitted intensity field was azimuthally independent, as predicted by theory for optically thick clouds, and integrated the CAR measurements over zenith angle to obtain estimates of the spectral fluxes in the upward and downward hemispheres. Table 2 summarizes the spectral surface reflectivities and corresponding standard deviations obtained from this analysis for all 13 channels of the CAR. These measurements represent, to the best of our knowledge, the first spectral reflectivity measurements of the ocean surface under cloudy conditions. Our measurements in the energetic portion of the visible spectrum are ~0.066, decreasing to ~0.040 at 2.20

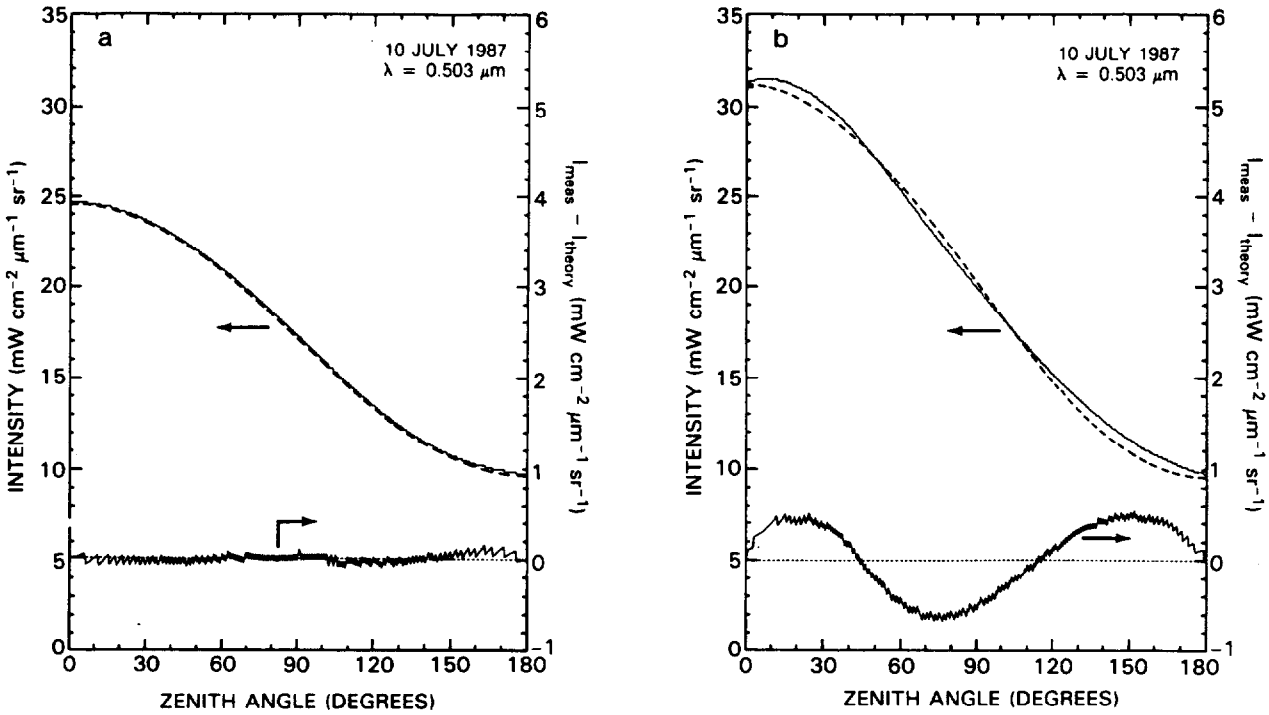

FIG. 8. Intensity as a function of zenith angle for two scans of the cloud absorption radiometer. Superimposed on the measurements (continuous curve) is the theoretical cosine function (dashed curve) necessary for the measurements to be within the diffusion domain. The right-hand scale applies to the deviations between measurements and theory, illustrated in the lower portion of each panel. The scan on the left (a) satisfies all conditions of the diffusion domain criteria (dashed and continuous curves coincide), whereas the scan on the right (b) fails to satisfy these criteria. All measurements were made at $\lambda = 0.503$ μm.

μm, in close agreement with the broadband shortwave ocean reflectivity measurements of 0.061, reported by Payne (1972).

In addition to the spectral cloud radiation measurements discussed above, the University of Washington's C-131A research aircraft contained broadband shortwave upward- and downward-looking pyranometers, cloud microphysics probes, an air batch sampler for measuring the size distribution of cloud interstitial aerosol, and a counterflow virtual impactor for measuring the light absorbing material within the cloud droplets. Detailed descriptions of these instruments can be found in Coulson (1975), Knollenberg (1981), Radke (1983), and Noone et al. (1988), respectively.

Figure 9 illustrates the average cloud droplet size distribution measured during the time period of the cloud absorption radiometer measurements presented in Fig. 7. These measurements were obtained using

TABLE 2. Ocean reflectivity (A_g), asymmetry factor (g), and optical thickness ($\tau_c - \tau$) for the marine stratocumulus cloud of 10 July 1987.

Optical channel	Wavelength (μm)	Ocean reflectivity	Asymmetry factor	Optical thickness
1	0.503	0.0742 ± 0.0079	0.8579	12.63 ± 2.09
2	0.673	0.0606 ± 0.0076	0.8517	12.78 ± 2.11
3	0.744	0.0634 ± 0.0078	0.8494	12.85 ± 2.12
4	0.866	0.0608 ± 0.0078	0.8454	12.94 ± 2.14
5	1.031	0.0555 ± 0.0079	0.8398	13.07 ± 2.16
6	1.198	0.0500 ± 0.0082	0.8351	13.18 ± 2.18
7	1.247	0.0542 ± 0.0085	0.8331	13.18 ± 2.18
8	1.547	0.0432 ± 0.0151	0.8288	13.51 ± 2.27
9	1.640	0.0426 ± 0.0086	0.8246	13.52 ± 2.28
10	1.722	0.0389 ± 0.0045	0.8202	13.37 ± 2.26
11	1.996	0.0440 ± 0.0165	0.8205	13.94 ± 2.11
12	2.200	0.0404 ± 0.0120	0.8093	13.84 ± 2.40
13	2.289	0.0804 ± 0.0097	0.8078	13.99 ± 2.25

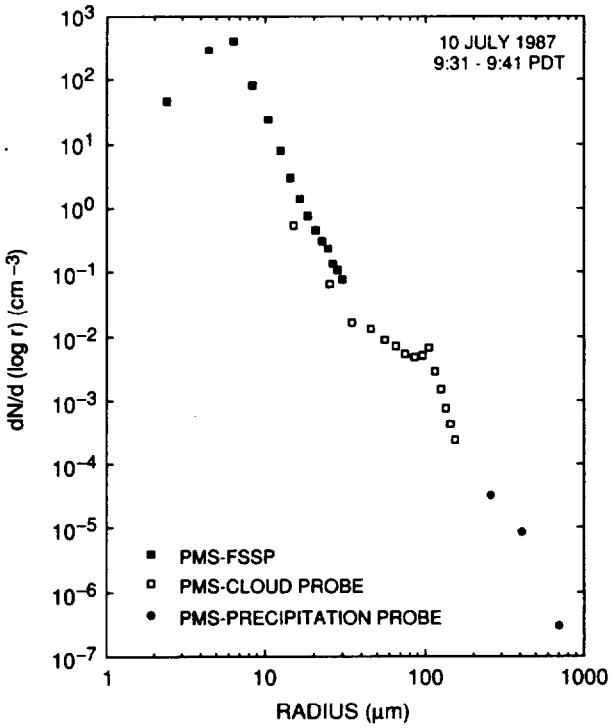

FIG. 9. Average cloud droplet size distribution for the 50 km section of marine stratocumulus clouds on 10 July 1987. The data points represent measurements made with a PMS FSSP-100 (solid squares), PMS OAP-200X cloud probe (open squares), and a PMS OAP-200Y precipitation probe (solid circles).

three different PMS cloud physics probes, the FSSP-100 (solid squares), OAP-200X cloud probe (open squares), and OAP-200Y precipitation probe (solid circles). This droplet size distribution has a noticeable drizzle mode at a radius of around 100 μm, a characteristic that was frequently observed during the FIRE marine stratocumulus IFO (Albrecht 1989; Radke et al. 1989). The effective radius (r_e) computed from this distribution is 7.15 μm.

Before applying the diffusion domain method to the experimental observations presented in Fig. 7, it was first necessary to calculate the relative optical thickness, asymmetry factor, single scattering albedo, and similarity parameter of water clouds as a function of wavelength for the cloud layer having the measured cloud droplet size distribution of Fig. 9. Unlike the results presented in Figs. 1–4, these computations required a blend of Mie theory for size parameters ($2\pi r/\lambda$) less that 100 and complex angular momentum (CAM) theory (Nussenzveig and Wiscombe 1980) for size parameters greater than 100. The use of CAM theory was necessitated by the fact that the measured droplet size distribution contained an appreciable number of drizzle droplets having radii much greater than typically included in the modified gamma distribution, radii that would otherwise be prohibitively expensive to include in Mie theory computations. Furthermore, these calculations were performed using a logarithmic, rather than linear, integration over the size distribution. The asymmetry factor derived from the measured size distribution is summarized in Table 2 for all wavelengths of the CAR.

The scaled optical thickness between the aircraft flight level and the base of the clouds was derived by applying Eq. (10) to all scan lines of Fig. 7 that satisfied the diffusion domain criteria. Figure 10 illustrates the optical thickness $\tau_c - \tau$ as a function of distance, where we converted scaled optical thickness to optical thickness using the asymmetry factor $g = 0.8579$ applicable to this wavelength ($\lambda = 0.503$ μm). Of the 1000 scan lines presented in Fig. 7, 611 passed the restrictive selection criteria discussed in section 4. Among those measurements excluded from our analysis were the optically thin scans at the beginning of the time series and the measurements that were contaminated by the sun (at distances of 24.9 and 28.0 km). As expected, the measurements between 11.5 and 19.4 km that had a relatively low zenith intensity and relatively high nadir intensity correspond to a region of large optical thickness beneath the aircraft. Table 2 summarizes the mean and standard deviation of the optical thickness obtained from this analysis for channel 1, together with corresponding results at the other channels obtained by applying the relative optical thickness predicted from calculations using the measured cloud droplet size distribution.

Given the surface reflectivity and optical thickness (or scaled optical thickness) of an individual scan at a specified wavelength, the intensity ratio $I(\tau, -1)/I(\tau, 1)$ is reduced solely to a function of similarity parameter s. Utilizing Eq. (5), together with the similarity relations of Table 1, we were thus able to calculate the intensity ratio as a function of similarity parameter and match this functional relationship with the measured intensity ratio to derive a value of the similarity parameter for a given measurement and wavelength.

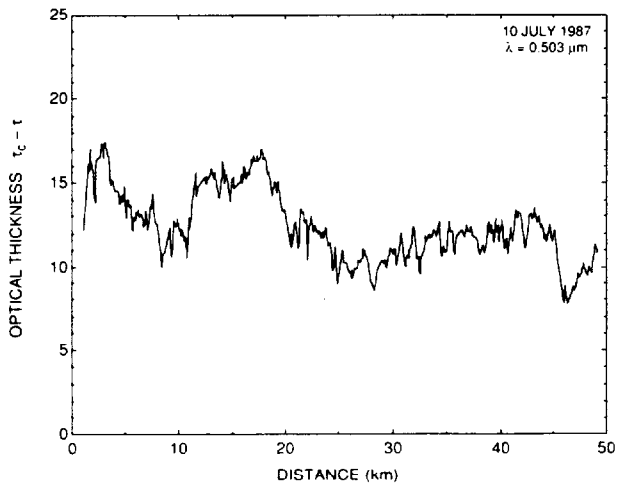

FIG. 10. Optical thickness beneath the aircraft for all measurements of Fig. 7 that satisfy the diffusion domain criteria. These results were derived from measurements at $\lambda = 0.503$ μm.

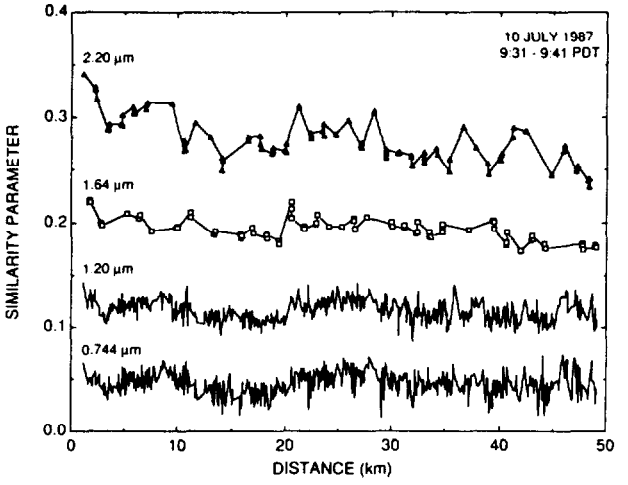

FIG. 11. Similarity parameter as a function of distance for four wavelengths of the cloud absorption radiometer.

Figure 11 illustrates the similarity parameter as a function of distance for four wavelengths of the CAR determined in this manner. The tendency for the similarity parameter to decrease with increasing distance, especially noticeable at 1.64 and 2.20 μm, is due to a modest decrease in the effective radius of the cloud droplets over this distance and not to a decrease in the imaginary part of the complex refractive index of the cloud droplets themselves. Due to the use of a filter wheel to measure the intensity field in channels 8–13, diffusion domain measurements were obtained in this time interval for between 71 and 87 scans, depending on filter position, in contrast to 611 for the first seven simultaneously sampled channels.

Figure 12 illustrates the mean and standard deviation of the spectral similarity parameter for all thirteen channels of the CAR obtained from aircraft measurements on 10 July 1987. Although the conversion from s to ω_0 is not unique, due to the moderate spectral variation of g, we have provided a single scattering albedo scale in this figure as a matter of convenience. This scale, shown on the right-hand side of Fig. 12, is strictly applicable at $\lambda = 0.754$ μm. Based on profile ascents and descents following these measurements, the stratocumulus cloud layer was determined to be 440 m thick with a cloud base at 490 m.

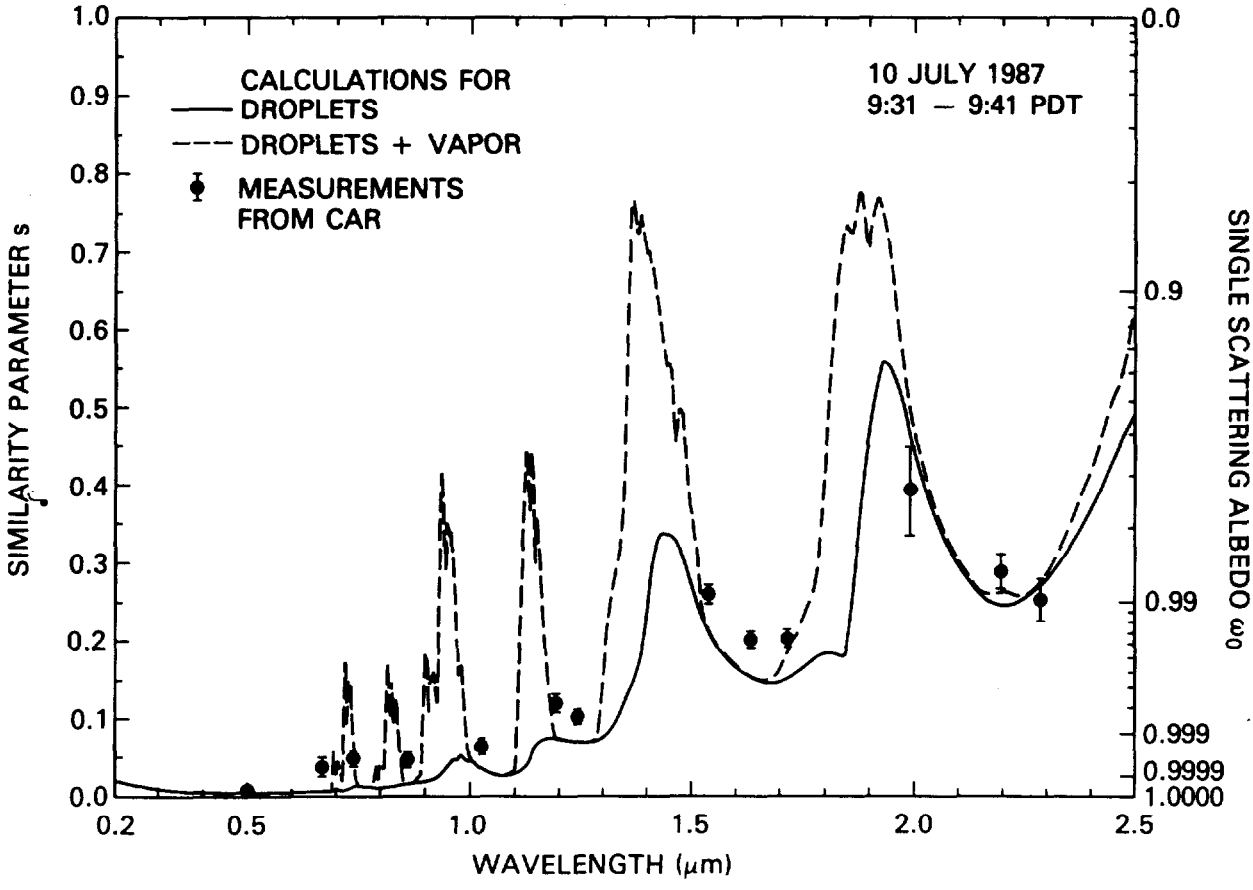

FIG. 12. Calculations of the similarity parameter as a function of wavelength for water droplets alone (solid line) and drops plus vapor (dashed line) for the cloud droplet size distribution and water vapor conditions of the marine stratocumulus cloud of 10 July 1987. The single scattering albedo scale is valid at $\lambda = 0.754$ μm, where the cloud asymmetry factor $g = 0.848$. The measurements derived from the cloud absorption radiometer (solid circles with error bars) are averages of the similarity parameter derived by applying the diffusion domain method to the 50 km section of this cloud.

In addition to the experimental results obtained using the CAR, Fig. 12 illustrates calculations of the similarity parameter as a function of wavelength for a cloud composed of water droplets only (solid curve) and droplets plus saturated vapor at 10.3°C (dashed curve). The water droplet computations were again based on a combination of Mie theory and complex angular momentum theory applied to the measured cloud droplet size distribution of Fig. 9. The water vapor computations, on the other hand, were based on assuming the cloud to be composed of saturated vapor and applying the necessary pressure and temperature scaling to obtain an equivalent absorber amount (w = 0.41 g cm^{-2}). The water vapor transmission functions were then computed for this cloud layer at a resolution of 20 cm^{-1} using LOWTRAN 5 (Kneizys et al. 1980). The absorption optical depths thus obtained were combined with the corresponding optical properties for cloud droplets, where we further assumed that the total cloud optical thickness τ_c = 16 at a wavelength of 0.754 μm.

These results show that, *in this case,* the measured absorption of solar radiation by clouds is close to, but persistently larger than, theoretical calculations. Furthermore, these findings support the view that clouds absorb more and reflect less solar radiation than theoretical predictions. Comparing Figs. 4 and 12 we see that a somewhat better agreement between measurements and theory could be achieved for $\lambda \leqslant 1.722$ μm by postulating an effective radius $\sim$ 45% larger than that of the cloud droplet size distribution than was observed. However, this would result in less absorption than theory for longer wavelengths, where the agreement is already quite remarkable. For example, the measured similarity parameter at 2.20 μm is consistent with an r_e of 7.36 μm, a value that is only 3% larger than the observed value of 7.15 μm. Thus we are unable to bring theory and measurements into complete agreement by simply postulating an error in the measurement of r_e, as this would improve the agreement in some parts of the spectrum and worsen the agreement in other parts of the spectrum.

Table 3 summarizes the spectral similarity parameter (and corresponding single scattering albedo) for all 13 wavelengths of the CAR, together with theoretical calculations for the measured droplet size distribution for this day. Based on these results we are forced to conclude that our observations provide additional evidence for the existence of "anomalous absorption," as discussed by Stephens et al. (1978), Twomey and Cocks (1982), Foot (1988), and Stephens and Tsay (1989), but that our observations of excess absorption are small in the marine stratocumulus cloud that we sampled on 10 July 1987.

Twomey (1977) suggested that anomalous absorption might be due to contamination of cloud droplets by pollutants. On 7–10 July 1987, the large-scale synoptic situation was unfavorable for the transport of continental pollution to the region of our observations. The low-level flow over the eastern Pacific Ocean was dominated by an unusually strong (100.5 kPa) thermal trough of low pressure over the interior of California, and a moderate (103 kPa) semipermanent, high-pressure area was centered $\sim$3000 km to the west of the region where our measurements were made. This pressure pattern produced strong northwesterly winds at the surface with an onshore component along the West Coast of the United States. A detailed air parcel trajectory analysis was carried out using horizontal and vertical winds from the European Centre for Medium-Range Weather Forecasts' gridded hemispheric dataset. Back trajectories for air parcels above (85.0 kPa), within (90.0 kPa) and below (96.0 kPa) the cloud layer we sampled all ran rapidly north, well clear of the California coast, and then, from a point off the northern Oregon coast, they turned WSW into the central Pacific

TABLE 3. Measured and theoretical values of the spectral similarity parameter and single scattering albedo of the marine stratocumulus cloud of 10 July 1987.

Optical channel	Wavelength (μm)	Similarity parameter		Single scattering albedo	
		Measurements	Theory	Measurements	Theory
1	0.503	0.0005 ± 0.0029	0.0009	1.00000 ± 0.00000	1.00000*
2	0.673	0.0359 ± 0.0125	0.0044	0.99981 ± 0.00013	1.00000*
3	0.744	0.0456 ± 0.0104	0.0259	0.99969 ± 0.00014	0.99990
4	0.866	0.0449 ± 0.0104	0.0146	0.99969 ± 0.00014	0.99997
5	1.031	0.0606 ± 0.0101	0.0326	0.99941 ± 0.00020	0.99983
6	1.198	0.1154 ± 0.0100	0.0738	0.99778 ± 0.00039	0.99910
7	1.247	0.0979 ± 0.0092	0.0684	0.99839 ± 0.00030	0.99922
8	1.547	0.2523 ± 0.0127	0.2062	0.98850 ± 0.00123	0.99246
9	1.640	0.1937 ± 0.0111	0.1527	0.99321 ± 0.00080	0.99583
10	1.722	0.1957 ± 0.0109	0.1947	0.99290 ± 0.00082	0.99297
11	1.996	0.3810 ± 0.0574	0.4822	0.97042 ± 0.01012	0.94842
12	2.200	0.2772 ± 0.0217	0.2631	0.98438 ± 0.00261	0.98602
13	2.289	0.2444 ± 0.0284	0.2780	0.98794 ± 0.00294	0.98415

* Rounded to six significant figures, not exact.

Ocean. At the highest pressure level we calculated (70.0 kPa), the initial transport was rather slow but it followed a similar path.

On a smaller scale, a Catalina eddy (Bosart 1983) dominated the circulation along the Southern California coast and this created a potential for transporting pollution from the land to the region of our observations. However, aerosol measurements made aboard the C-131A aircraft indicated rather clean maritime air. Beneath the cloud deck, the volume scattering coefficient due to dry particles was $\sim 2 \times 10^{-6}$ m^{-1} and the Aitken nucleus concentrations were 200–300 cm^{-3}. Above the clouds, the same clean conditions prevailed for 100–200 m, followed by a layer of modest pollution about 100–200 m thick and then clean air again above that level. Measurements with a counterflow virtual impactor (CVI) were also made aboard the aircraft. Throughout the FIRE project we detected only small quantities of soot (3–88 ng of soot per gram of cloud water). Unfortunately, measurements with the CVI were not obtained on 10 July, but on 7 July, in a similar meteorological regime to that on 10 July, we measured the lowest values during FIRE (3 ng of soot per g of cloud water). Cloud interstitial measurements of absorption by soot, obtained using the integrating plate technique (Weiss and Waggoner 1984; Radke 1983), were below detection limits ($\sim 2 \times 10^{-7}$ m^{-1}) on 10 July and on all the other days on which measurements were obtained during FIRE, some of which included days with a modest continental influence. Twohy et al. (1989) calculated that the absorption of solar radiation by these concentrations of soot should be negligible.

Hence, on 10 July 1987, when our measurements showed small but detectable levels of anomalous absorption by marine stratocumulus clouds off the coast of Southern California, neither the air nor the cloud water should have been appreciably affected by either natural or anthropogenic sources of particles or gases from the North American mainland.

6. Summary and conclusions

In this paper we have presented results of the first experimental application of the diffusion domain method to the determination of the spectral similarity parameter, and hence the single scattering albedo, of clouds. In this method, airborne measurements of the relative angular distribution of scattered radiation are compared to known asymptotic expressions for the intensity field deep within an optically thick cloud layer. Analytic expressions relating the ratio of the nadir-to-zenith intensities to surface reflectivity (A_g), similarity parameter (s), and scaled optical thickness beneath the aircraft flight level [$(1 - g)(\tau_c - \tau)$] have been used to analyze measurements obtained with a multiwavelength scanning radiometer (King et al. 1986) mounted in the nose of the University of Washington C-131A research aircraft.

The principal assumption on which the diffusion domain method is based is that the cloud is nonabsorbing at some wavelength in the visible region. This assumption permits the scaled optical thickness between the aircraft flight level and the base of the cloud to be derived using the asymptotic expression for the internal intensity ratio deep within an optically thick, conservatively scattering, atmosphere, thereby making it unnecessary to have ancillary measurements or an absolute calibration of the radiometer. Figure 10 shows an example of the optical thickness beneath the aircraft derived in this manner for a 50 km section of marine stratocumulus cloud some 355 km off the coast of San Diego on 10 July 1987, where the conversion from scaled optical thickness to optical thickness was based on the asymmetry factor calculated from the measured cloud droplet size distribution (cf. Fig. 9).

To apply the diffusion domain method to experimental observations, it is necessary to determine whether the observations are made far enough from the top and bottom boundaries of a sufficiently thick cloud to be within the diffusion domain, defined as a region where the diffuse radiation field assumes an asymptotic form characterized by rather simple properties. This may be accomplished by comparing the measured intensity as a function of zenith angle with that expected from theory for a nonabsorbing or weakly absorbing wavelength. Figure 8 provides an illustration of the use of the complete angular distribution of scattered radiation to determine the measurements within the diffusion domain. This figure provides an example of both a satisfactory (Fig. 8a) and unsatisfactory (Fig. 8b) scan, where the latter measurements were obtained too high in the cloud and were thus influenced by the solar aureole maximum away from the zenith.

The measurements presented in this article were obtained in a layer of clean marine stratocumulus clouds approximately 440 m thick and over 150 km in horizontal extent. The spectral reflectivity of the underlying ocean surface was determined from aircraft measurements with the CAR beneath the cloud layer. Having determined the scans that contain diffusion domain measurements, and having derived the spectral surface reflectivity as well as the scaled optical thickness beneath the aircraft, the similarity parameter was derived at the remaining twelve channels of the radiometer. This analysis required the variation of the scaled optical thickness with wavelength to be taken into account, and was accomplished by using the relative variation of scaled optical thickness derived from calculations using the measured cloud droplet size distribution.

Once the spectral variation of A_g and $(1 - g)(\tau_c - \tau)$ was included in our analysis, the spectral similarity parameter was determined, as demonstrated in Fig. 12 and summarized in Table 3. The theoretical calculations presented in Fig. 12 were based on a 440 m thick cloud composed of saturated vapor at 10.3°C and water droplets having the measured cloud droplet size dis-

tribution of 10 July 1987. The close agreement between measurements and theory in this case, where our measurements show a small but consistently larger absorption than theoretical predictions, is not inconsistent with modest "anomalous absorption" in these clouds that were largely free of anthropogenic influence. The single scattering albedos that we obtained from our analysis in the visible wavelength region, though somewhat lower than theory, are still ~0.9999, values generally much too large to be able to explain any reduced reflection by these clouds ($15 \leqslant \tau_c \leqslant 20$). On the other hand, in the wavelength region between 1.6 and 2.2 μm, our measurements of excess absorption are consistent with the observations of Twomey and Cocks (1982), Stephens and Platt (1987), and Foot (1988), who reported unusually low spectral reflectance in this wavelength region. An examination of other single and multiple aircraft missions to study marine stratocumulus clouds in FIRE will be reported in future contributions.

Acknowledgments. We are grateful to Drs. T. Nakajima and J. S. Foot for valuable comments and numerous discussions concerning the research techniques, and to H. G. Meyer for programming contributions and much needed assistance in data analysis. The research reported in this article has been supported by NASA's Climate Program and the National Science Foundation under Grant ATM-8615344.

REFERENCES

Albrecht, B. A., 1989: Aerosols, cloud microphysics, and fractional cloudiness. *Science,* **245,** 1227–1230.

——, D. A. Randall and S. Nicholls, 1988: Observations of marine stratocumulus clouds during FIRE. *Bull. Amer. Meteor. Soc.,* **69,** 618–626.

Bosart, L. F., 1983: Analysis of a California Catalina eddy event. *Mon. Wea. Rev.,* **111,** 1619–1633.

Cess, R. D., G. L. Potter, J. P. Blanchet, G. J. Boer, S. J. Ghan, J. T. Kiehl, H. Le Treut, Z. X. Li, X. Z. Liang, J. F. B. Mitchell, J. J. Morcrette, D. A. Randall, M. R. Riches, E. Roeckner, U. Schlese, A. Slingo, K. E. Taylor, W. M. Washington, R. T. Wetherald and I. Yagai, 1989: Interpretation of cloud-climate feedback as produced by 14 atmospheric general circulation models. *Science,* **245,** 513–516.

Coulson, K. L., 1975: *Solar and Terrestrial Radiation.* Academic Press, 322 pp.

Cox, S. K., D. S. McDougal, D. A. Randall and R. A. Schiffer, 1987: FIRE—The First ISCCP Regional Experiment. *Bull. Amer. Meteor. Soc.,* **68,** 114–118.

Davies, R., W. L. Ridgway and K. E. Kim, 1984: Spectral absorption of solar radiation in cloudy atmospheres: A 20 cm^{-1} model. *J. Atmos. Sci.,* **41,** 2126–2137.

Downing, H. D., and D. Williams, 1975: Optical constants of water in the infrared. *J. Geophys. Res.,* **80,** 1656–1661.

Foot, J. S., 1988: Some observations of the optical properties of clouds. I: Stratocumulus. *Quart. J. Roy. Meteor. Soc.,* **114,** 129–144.

Hale, G. M., and M. R. Querry, 1973: Optical properties of water in the 200-nm to 200-μm wavelength region. *Appl. Opt.,* **12,** 486–492.

Hansen, J. E., 1971: Multiple scattering of polarized light in planetary atmospheres. Part II. Sunlight reflected by terrestrial water clouds. *J. Atmos. Sci.,* **28,** 1400–1426.

——, and L. D. Travis, 1974: Light scattering in planetary atmospheres. *Space Sci. Rev.,* **16,** 527–610.

Herman, G. F., 1977: Solar radiation in summertime arctic stratus clouds. *J. Atmos. Sci.,* **34,** 1423–1432.

——, and J. A. Curry, 1984: Observational and theoretical studies of solar radiation in arctic stratus clouds. *J. Climate Appl. Meteor.,* **23,** 5–24.

Hignett, P., 1987: A study of the shortwave radiative properties of marine stratus: Aircraft measurements and model comparisons. *Quart. J. Roy. Meteor. Soc.,* **113,** 1011–1024.

King, M. D., 1981: A method for determining the single scattering albedo of clouds through observation of the internal scattered radiation field. *J. Atmos. Sci.,* **38,** 2031–2044.

——, 1987: Determination of the scaled optical thickness of clouds from reflected solar radiation measurements. *J. Atmos. Sci.,* **44,** 1734–1751.

——, and Harshvardhan, 1986: Comparative accuracy of selected multiple scattering approximations. *J. Atmos. Sci.,* **43,** 784–801.

——, M. G. Strange, P. Leone and L. R. Blaine, 1986: Multiwavelength scanning radiometer for airborne measurements of scattered radiation within clouds. *J. Atmos. Oceanic Technol.,* **3,** 513–522.

Kneizys, K. X., E. P. Shettle, W. O. Gallery, J. H. Chetwynd, L. W. Abreu, J. E. A. Selby, R. W. Fenn and R. A. McClatchey, 1980: Atmospheric transmittance/radiance: Computer code LOWTRAN 5. AFGL-TR-80-0067, Air Force Geophysics Laboratories, Hanscom AFB, 233 pp.

Knollenberg, R. G., 1981: Techniques for probing cloud microstructure. *Clouds: Their Formation, Optical Properties, and Effects,* P. V. Hobbs and A. Deepak, Eds., Academic Press, 15–91.

Noone, K. J., R. J. Charlson, D. S. Covert, J. A. Ogren and J. E. Heintzenberg, 1988: Design and calibration of a counterflow virtual impactor for sampling of atmospheric fog and cloud droplets. *Aerosol Sci. Tech.,* **8,** 235–244.

Nussenzveig, H. M., and W. J. Wiscombe, 1980: Efficiency factors in Mie scattering. *Phys. Rev. Lett.,* **45,** 1490–1494.

Palmer, K. F., and D. Williams, 1974: Optical properties of water in the near infrared. *J. Opt. Soc. Amer.,* **64,** 1107–1110.

Payne, R. E., 1972: Albedo of the sea surface. *J. Atmos. Sci.,* **29,** 959–970.

Radke, L. F., 1983: Preliminary measurements of the size distribution of cloud interstitial aerosol. *Precipitation Scavenging, Dry Deposition and Resuspension,* H. R. Pruppacher, R. G. Semonin and W. G. N. Slinn, Eds., Elsevier, 71–78.

——, J. A. Coakley, Jr. And M. D. King, 1989: Direct and remote sensing observations of the effects of ships on clouds. *Science,* in press.

Ramanathan, V., 1987: The role of earth radiation budget studies in climate and general circulation research. *J. Geophys. Res.,* **92,** 4075–4095.

——, R. D. Cess, E. F. Harrison, P. Minnis, B. R. Barkstrom, E. Ahmad and D. Hartmann, 1989: Cloud-radiative forcing and climate: Results from the Earth Radiation Budget Experiment. *Science,* **243,** 57–63.

Reynolds, D. W., T. H. Vonder Haar and S. K. Cox, 1975: The effect of solar radiation absorption in the tropical troposphere. *J. Appl. Meteor.,* **14,** 433–444.

Rozenberg, G. V., M. S. Malkevich, V. S. Malkova and V. I. Syachinov, 1974: Determination of the optical characteristics of clouds from measurements of reflected solar radiation on the Kosmos 320 satellite. Izv. Acad. Sci. USSR, *Atmos. Ocean. Phys.,* **10,** 14–24.

Slingo, A., 1989: A GCM parameterization for the shortwave radiative properties of water clouds. *J. Atmos. Sci.,* **46,** 1419–1427.

——, and H. M. Schrecker, 1982: On the shortwave radiative properties of stratiform water clouds. *Quart. J. Roy. Meteor. Soc.,* **108,** 407–426.

Stephens, G. L., and C. M. R. Platt, 1987: Aircraft observations of

the radiative and microphysical properties of stratocumulus and cumulus cloud fields. *J. Climate Appl. Meteor.*, **26**, 1243–1269.
——, and S. C. Tsay, 1989: On the cloud absorption anomaly. *Quart. J. Roy. Meteor. Soc.*, in press.
——, G. W. Paltridge and C. M. R. Platt, 1978: Radiation profiles in extended water clouds. III: Observations. *J. Atmos. Sci.*, **35**, 2133–2141.
——, S. Ackerman and E. A. Smith, 1984: A shortwave parameterization revised to improve cloud absorption. *J. Atmos. Sci.*, **41**, 687–690.
Twohy, C. H., A. D. Clarke, S. G. Warren, L. F. Radke and R. J. Charlson, 1989: Light-absorbing material extracted from cloud droplets and its effect on cloud albedo. *J. Geophys. Res.*, **94**, 8623–8631.
Twomey, S., 1976: Computations of the absorption of solar radiation by clouds. *J. Atmos. Sci.*, **33**, 1087–1091.
——, 1977: The influence of pollution on the shortwave albedo of clouds. *J. Atmos. Sci.*, **34**, 1149–1152.
——, 1983: Radiative effects in California stratus. *Contrib. Atmos. Phys.*, **56**, 429–439.
——, and T. Cocks, 1982: Spectral reflectance of clouds in the near-infrared: Comparison of measurements and calculations. *J. Meteor. Soc. Japan*, **60**, 583–592.
van de Hulst, H. C., 1968: Asymptotic fitting, a method for solving anisotropic transfer problems in thick layers. *J. Comput. Phys.*, **3**, 291–306.
——, 1980: *Multiple Light Scattering. Tables, Formulas, and Applications*, Vols. 1 and 2. Academic Press, 739 pp.
Weiss, R. E., and A. P. Waggoner, 1984: Aerosol optical absorption: Accuracy of filter measurements by comparison with in situ extinction. *Aerosols: Science, Technology, and Industrial Applications of Airborne Particles*, B. Y. H. Liu, Ed., Elsevier, 397–400.
Wiscombe, W. J., R. M. Welch and W. D. Hall, 1984: The effects of very large drops on cloud absorption. Part I: Parcel models. *J. Atmos. Sci.*, **41**, 1336–1355.